Performance Predictions and Topology Improvements for Optical Serrodyne Comb Generators

Arthur Lowery, *Senior Member, IEEE*

***Abstract*—Detailed simulations identify which optical components affect the performance of a radio frequency (RF) and optical comb generator based on an optical loop with a phase modulator. The simulations suggest that the topology of the loop can be modified to give a flatter RF spectrum and a greater resilience to fluctuations in the optical phase length of the loop. Furthermore, a method of filtering the laser's output to reduce the noise floor of the RF comb is proposed and verified. The simulations show that the linewidth of the source is critical to good performance, as are the quality of the sawtooth and the short-term phase stability of the loop. However, the amplified spontaneous emission noise (ASE) from the optical amplifier within the loop is relatively unimportant.**

***Index Terms*—Microwave generation, optical delay lines, oscillator noise, semiconductor lasers, signal generators.**

I. Introduction

OPTICAL frequency combs locked to a radio frequency (RF) reference are useful as wavelength references in dense-wavelength-division-multiplexing systems [1], as millimeter-wave RF synthesizers [2], and when detected, they generate RF spectral combs [3] that can be used for beamforming networks [4], [5]. One method of generating optical frequency combs is to incorporate a sine-driven phase modulator into a recirculating optical loop fed with a continuous-wave (CW) source, as proposed and analyzed theoretically in [6]. Owing to the multiple modulation sidebands created on each pass of the modulator, this will produce optical combs downshifted and upshifted from the frequency of the CW source, but with decaying amplitudes of the lines in the combs away from the source frequency [6]. Generating equal-amplitude lines on one side of the CW source requires serrodyne frequency shifting (a modulator driven with a sawtooth wave [7]), or a single-sideband modulator [8], within the recirculating loop. Recently, a loop incorporating a serrodyne modulator has generated over 51 RF tones with an electrical signal-to-noise ratio (SNR) > 20 dB and a spacing of 20 MHz [5]. An alternative approach of injecting optical pulses into the loop, rather than CW light, has been demonstrated in [9], with the advantage that the sawtooth can be replaced with a sinusoid (which is approximately a linear ramp where the pulses are). The periodic pulses naturally generate a comb of optical lines; however, additional serrodyne modulation extends the spectrum. Optical frequency lines spaced at 12.5 GHz have been generated over an optical bandwidth > 500 GHz using this technique [9].

Theoretical analysis has shown the impact of the sawtooth quality on optical performance [10], in particular, the need to maintain the harmonic content of the sawtooth waveform and a fast fall time. However, there are a number of design factors that could also affect the performance of sawtooth-based systems, and an investigation of these factors has yet to be published.

This paper uses time-domain numerical simulations to investigate the factors affecting the performance of serrodyne comb generators and proposes a new topology of coupling in and out of the loop to improve the quality of the RF spectrum. The simulations represent optical fields by their complex envelope, sampled at a rate of 1.28 THz. The samples are passed from component to component in a data-flow fashion. Each component is represented by a numerical model. Each optical model operates on the optical samples to represent the physics of the devices (such as by phase modulating the signals, or adding optical noise). The electrical models operate on real-value signals representing the sampled electrical waveforms. The simulations were performed with a commercial photonic circuit and systems simulator, allowing many topologies to be built and compared without recompiling code.

The paper first investigates the theory of a perfect comb generator and then simulates the factors affecting the performance of a practical system. Among the factors investigated are 1) the topology of the ring and strength of the optical coupling in and out of the ring; 2) the linewidth of the CW source; 3) the relative intensity noise (RIN) of the source and how optical filtering can reduce its effect; 4) the modulation waveform bandwidth; 5) the modulation waveform noise; 6) optical phase drift around the loop; and 7) the performance of the optical amplifier. The improvements to the comb generator are then discussed, followed by conclusions.

II. Serrodyne Theory

An optical frequency shift may be obtained by adding a continuous increase (or decrease) in phase to an optical signal,

Manuscript received July 29, 2004; revised March 31, 2005. This work was partly performed at VPIphotonics (a division of VPIsystems), Kew, Victoria, Australia (www.vpiphotonics.com).

The author is with the Department of Electrical and Computer Systems Engineering, Monash University, Clayton, Victoria 3800, Australia (e-mail: arthur.lowery@eng.monash.edu.au).

Digital Object Identifier 10.1109/JLT.2005.850810

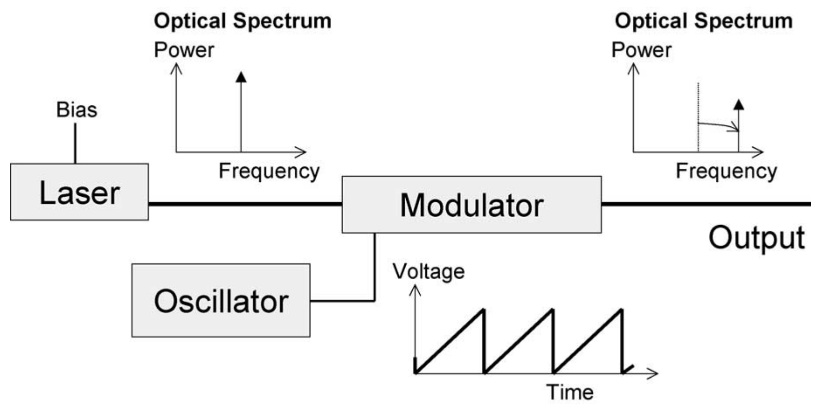

Fig. 1. Optical serrodyne modulation to frequency shift an optical line.

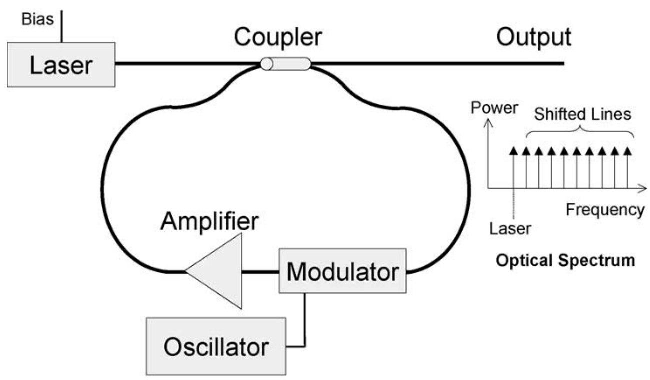

Fig. 2. Optical serrodyne modulator within a loop.

such as with a phase modulator driven by an ever increasing (or decreasing) voltage [7]. A phase ramp of 360 °/s will give a frequency increase of 1 Hz. However, an infinite phase ramp is obviously impractical, as an infinite power supply voltage would be required. Thus, a compromise is to drive the phase modulator with a sawtooth, which periodically flies back to its initial output, as shown in Fig. 1. During the flyback periods, a reverse frequency shift will occur, far exceeding the desired frequency shift. Furthermore, because the bandwidth of the sawtooth signal will be limited by the electronics of the oscillator, wiring, and modulator, the transition between ramp-up and flyback will be rounded, leading to a range of unwanted frequency shifts. Johnson and Cox [10] have analytically and experimentally studied the requirements on the sawtooth oscillator.

A. Serrodyne Modulation Within a Ring

If a serrodyne modulator is placed in an optical ring (such as a loop of fiber, as shown in Fig. 2), then the circulating energy will be shifted in optical frequency each time it passes through the modulator [5]. This is best explained by unwinding the path of the light within the loop as shown in Fig. 3, so that the horizontal axis represents time. The unwound path periodically has a laser (L), modulator (m), and output port. The graph in Fig. 3 shows the optical frequencies present in the loop. The laser injects at frequency f_0. When the laser's power reaches the modulator for the first time it is shifted to f_1. After further recirculation, it is shifted to f_2, and so on. However, a new laser is added to the loop, to be shifted on each circulation, until it is removed by the optical filter's stopband (not shown in the unwound loop). Thus, after four circulations, the loop will have filled with four spectral lines and will be in a steady state for this optical filter bandwidth. Note that to get to a given shifted line, the laser power always passes through an identical number of components along the path.

This explanation assumes that the laser source is monochromatic, the loop delay is locked to the repetition period, the frequency shifting is perfect, and that the system is noiseless. The remainder of the paper will look at the effects of real components on the system's performance.

B. Generation of an RF Comb

A comb of optical lines will produce a comb of RF tones upon photodetection [2], [7]. Each RF tone is the summation of the mixing products of many pairs of optical lines, except for the highest frequency that only has a contribution from the laser line and the most-shifted line. This summation of contributions means that lower frequency RF tones can be stronger than higher frequency tones, depending on the phases of the contributions. For maximum efficiency, the polarizations of the lines should be aligned. (Hereinafter, I will use the terminology optical *lines* and RF *tones* for clarity. The optical lines are either the *laser line* or a *shifted line*. The RF tones result from the summation of RF *contributions.*)

The phases of the contributions depend on the relative phases of the optical lines, which need to be tightly controlled to obtain an RF spectrum without nulls. Furthermore, the arrangement of Fig. 2 has a fundamental flaw: Because of the coupler, the direct path of the laser to the output will have a 180° phase shift relative to the light circulating the loop, if the loop is set up to be an integer number of optical wavelengths per circulation. This results in frequency nulls in the RF spectrum, because the contribution from the laser line mixing with a shifted line can cancel with the contributions from pairs of shifted lines. In reality, phase fluctuations around the loop, due to thermal expansion and mechanical vibration, will cause an average RF spectrum without nulls. However, each RF tone will have strong intensity fluctuations.

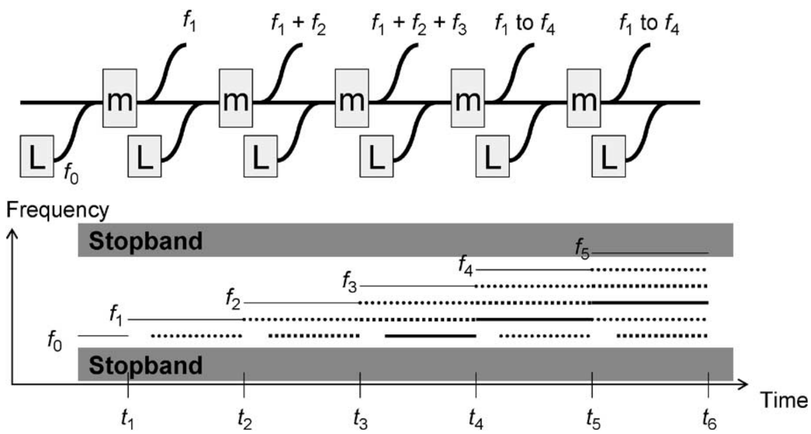

Fig. 3. Unwound model of the loop, where horizontal distance equates to time: L is the source laser (frequency f_0); m is the modulator. The optical filter is not shown, but its stopband removes frequency f_5. The output frequencies are plotted in the graph. The style of the lines indicates the shifting that occurs on each pass of the modulators.

C. New Topologies

A solution to the RF nulling problem is to redesign the loop with a more complex structure using two adjacent three-port couplers, one to inject the laser line into the loop and one to sample the loop's contents including the laser line. However, this results in a nonflat RF spectrum, where higher RF frequencies are attenuated, simply because more pairs of optical lines contribute to the lower frequency RF tones. A solution is to make the dominant contribution to an RF tone the beating between the laser line and one shifted line. This can be achieved by ensuring that the laser line is far stronger than any shifted line.

A filter could be used at the output of the loop to emphasize the laser line compared with the shifted lines. However, this would require a sharp cutoff and flat phase response, which are difficult to achieve together. An alternative coupler topology to mix a strong laser line with the shifted lines is shown in Fig. 4. Here, the laser's output is split into two parts, using a three-port coupler (coupler 3). One part is injected into the loop just before the amplifier and phase shifter. Thus, the laser line is always shifted before reaching the output coupler. The other part is mixed with the output of the loop, using a three-port coupler (coupler 4). The coupling ratios of the couplers can be arranged to ensure that the laser line is far stronger than any shifted line. The optimum-coupling ratio will be investigated by numerical simulation.

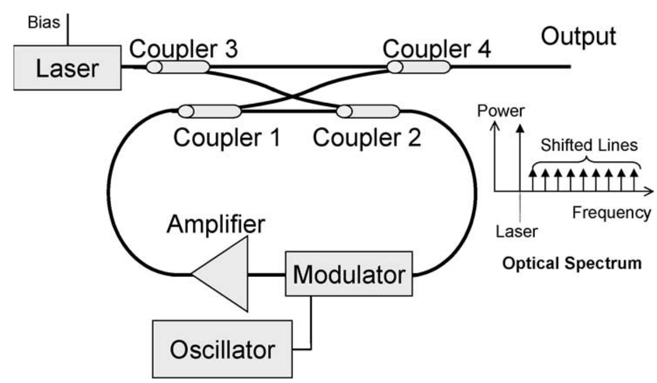

Fig. 4. Optical loop with four three-port couplers to achieve a strong laser line compared with the shifted lines.

III. Performance Simulations

Simulations have an advantage over laboratory prototypes in that the component parameters and optical phases can be set precisely. However, realistic parameters have to be entered into each component model to obtain realistic results. The simulation was performed with a commercial photonic system simulator, VPItransmissionMakerWDM.[1] This includes models of all of the components, suitable instrumentation, and a graphical design environment allowing the topology and parameters of the system to be specified easily. Furthermore, a set of signal processing modules allows arbitrary waveforms to be generated, in this case, a ramp waveform.

[1]VPItransmissionMakerWDM is a product of VPIphotonics (www.vpiphotonics.com), a division of VPIsystems Inc. (www.VPIsystems.com).

A. Simulation Setup

Fig. 5 shows the main simulation diagram. The laser can be represented by models of varying complexity [11]. The simplest "behavioral" model is for a CW laser with linewidth, a side mode, and a flat intensity noise, and will be used in this paper. A more complex "physical" model using rate equations for the photon and carrier densities within the laser can be used [12]. This would introduce nonflat intensity and frequency noise to represent the spectrum of the RIN and the lineshape more accurately. The simulation operates in the time domain. That is, the optical waveform is represented by an array of equally spaced samples [11]. Each sample represents the complex envelope of the optical signal at a given time. The bandwidth of the simulation was set to be 64 GHz, giving a timestep of 1/64 ns.

The modulator was initially assumed to be a perfect phase modulator, with a flat frequency response. The optical amplifier was set to compensate for the loss of the fiber loop and coupler exactly. The fiber loop was considered to be linear

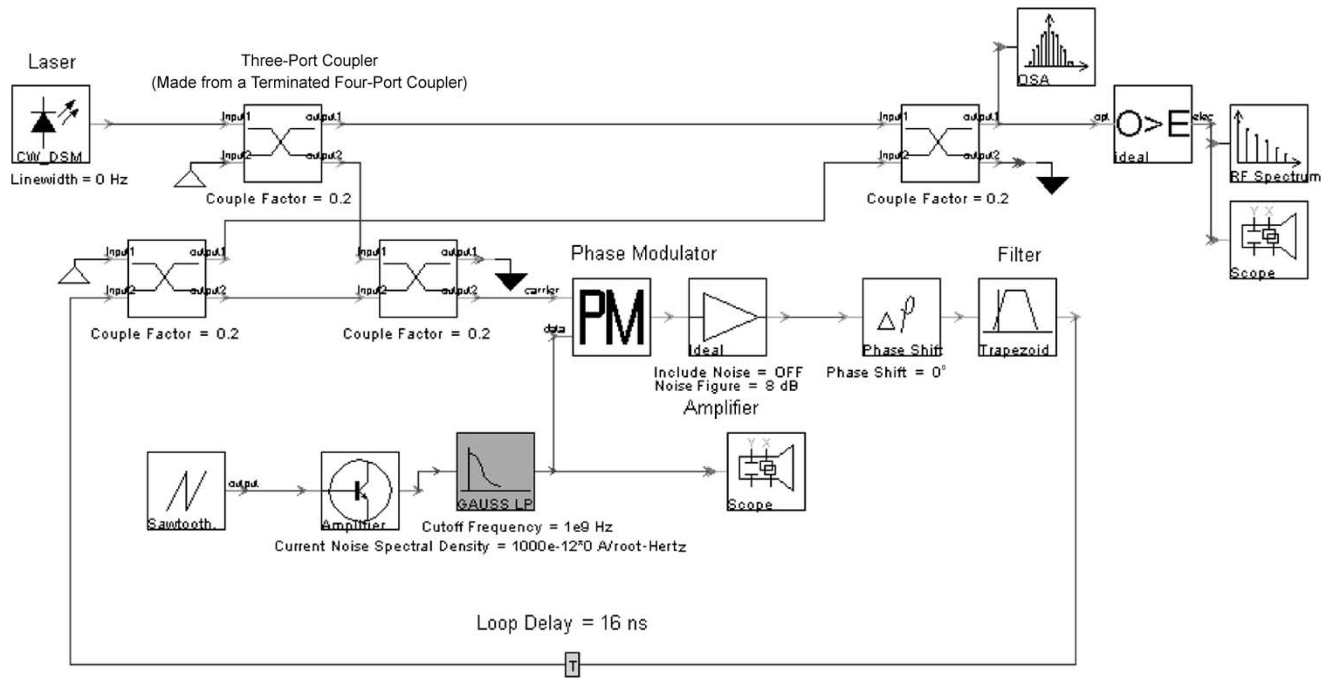

Fig. 5. Simulation schematic using VPItransmissionMaker.

and dispersionless. The delay of the loop was represented by a digital memory with a delay equal to exactly eight times the repetition period of the oscillator. The drive waveform was a perfect sawtooth. The optical filter was set to reject signals shifted by more than 20 shifts.

The frequency shift (hertz) is given by the 1/360 rate of change of optical phase (degree per second). The loop had a delay of 16 ns, and the modulator was driven over eight periods of 360° in 16 ns, using a 500-MHz sawtooth generator. Thus, the frequency shift was 8/16 ns or 500 MHz. This shift was chosen to fall exactly on the frequency grid of the simulator, to avoid spectral leakage when the spectrum was obtained using a Fourier transform. The resolution of the Fourier transform was 66 MHz. This system would require a high-quality sawtooth generator with harmonics extending beyond 16 GHz.

Fig. 6 shows the spectra of the output of the loop using these perfect assumptions after 19 recirculations. In the steady state, the CW laser signal becomes shifted beyond the 20-GHz passband of the optical filter after 25 recirculations.

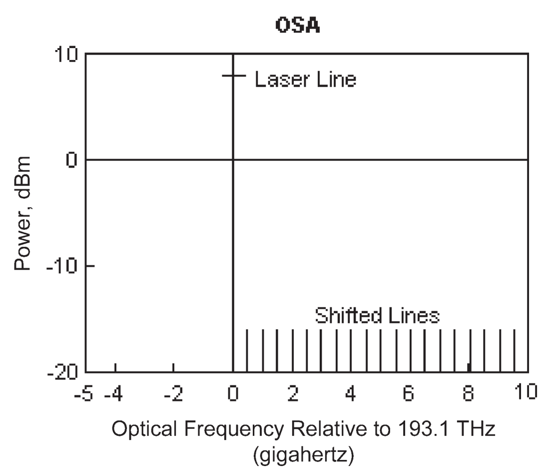

Fig. 6. Optical spectrum after 19 recirculations.

B. RF Spectrum and Coupler Strength

As described above, mixing of pairs of optical lines upon photodetection creates the RF spectrum. Ideally, there should be a dominant contribution to each RF tone from the laser line mixing with a single shifted line. This can be achieved using the arrangement in Fig. 5 with weak cross-coupling of the couplers (from the top to the bottom ports).

Fig. 7(a) and (b) shows the effect of varying this cross-coupling amount of 20% and 50%. The spectra have reached a steady state after 30 simulations in each case. The flattest RF spectrum ($<$ 6 dB variation to 10 GHz) is obtained with the weakest coupling [Fig. 7(a)], because the laser line at the output is approximately 26 dB stronger than the shifted lines, given by $10\log(\mathrm{coupling})^4$–amplifier gain–laser path loss), where the amplifier gain is $-10\log(1-\mathrm{coupling})^2$ and the laser path loss is $-10\log(\mathrm{coupling})^2$.

Strong coupling [50%, Fig. 7(b)] leads to equal powers of the laser line and the shifted line at the photodetector, however, there is $>$ 20 dB difference between the RF tones at 500 MHz and 10 GHz. An advantage of the 50% coupler, however, is the 11 dB more power in the 10-GHz tone than for the 20% coupling. This suggests that an electrical filter would be a better option to flatten the RF spectrum, and this would not require the coupler arrangement of Fig. 3. A later result will show that the 50% coupler option is more sensitive to phase drifts. Thus, a 20% coupling was used in all the remaining simulations.

Zero coupling of the laser line to the output was also tried (discarding the top two couplers. This system gave very strong RF powers (see Fig. 8), but also a large sensitivity to the relative phases of all the RF tones.

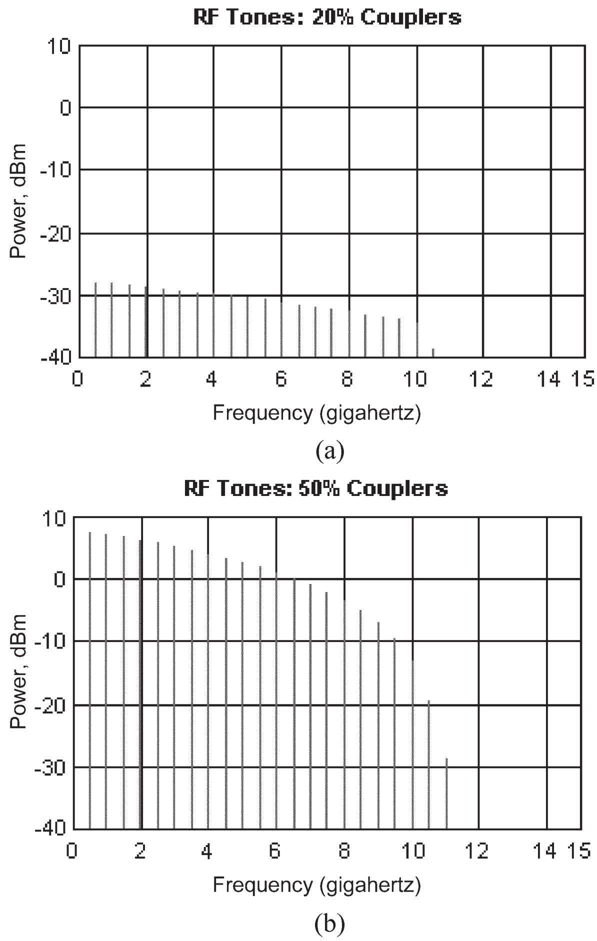

Fig. 7. (a) RF spectrum with 20% couplers. (b) RF spectrum with 50% couplers.

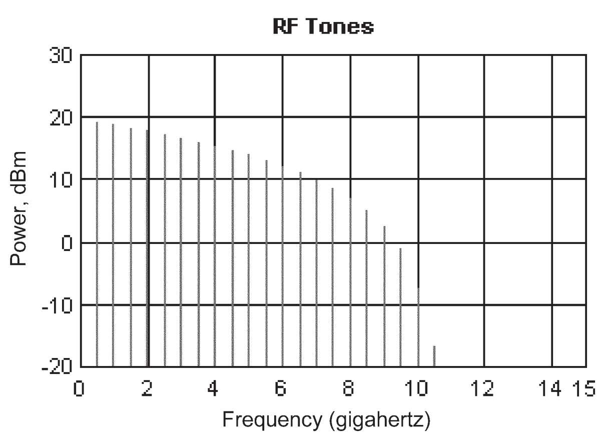

Fig. 8. RF spectrum with no coupler 3 and coupler 4 (no laser line at the output).

C. Laser Linewidth

The source linewidth was increased from 0 to 100 kHz, which is typical for an external-cavity laser. The lineshape was assumed to be Lorentzian for this simulation. Fig. 9 shows the RF spectrum after 30 recirculations. This has a noise floor approximately 40 dB down from the strongest RF tone. Increasing the linewidth to 10 MHz (a poor DFB laser) increased the noise floor by 20 dB (Fig. 10). This 1:1 scaling is similar to that simulated in signal processing systems with dispersive optical elements [11]. The linewidth has a significant impact because the shifted lines take their phase from earlier parts of the laser waveform than the laser line itself, as the loop is acting as a delay. Thus, the random walk of the laser's phase has to be accumulated over n recirculations for the nth RF tone to obtain the relative phase of the laser line and the shifted line to calculate the RF phase.

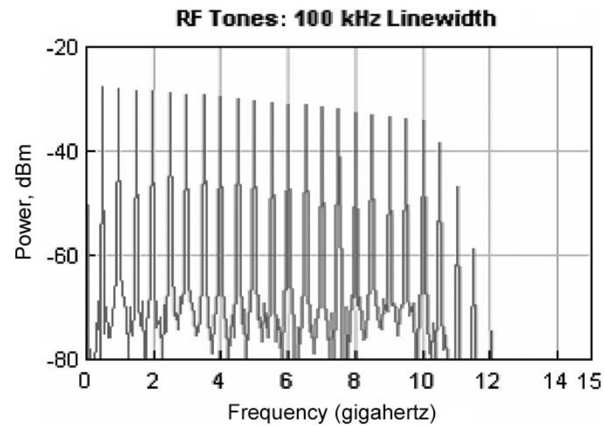

Fig. 9. RF spectrum for a 100-kHz linewidth laser.

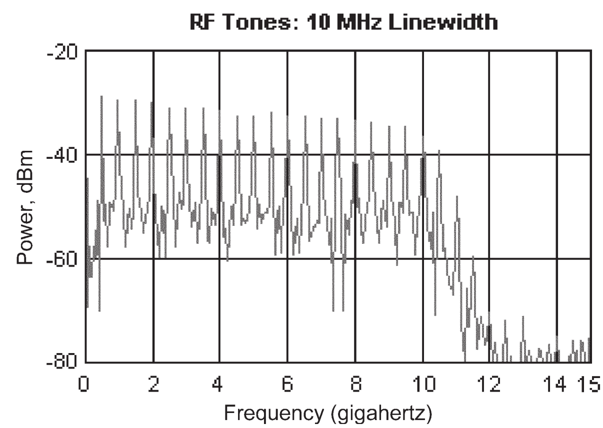

Fig. 10. RF spectrum for a 10-MHz linewidth laser.

D. Laser Intensity Noise (RIN)

Intensity noise causes optical noise sidebands around the laser line extending to tens of gigahertz, but with a peak around the laser's resonant frequency (5–20 GHz) [11]. These sidebands will mix with shifted laser lines at the photodiode to cause wide-band electrical noise. In these simulations, a flat RIN spectrum was assumed to get an upper bound on the tolerable RIN. The linewidth was reset to zero. Fig. 11 shows the optical spectrum, and Fig. 12 depicts the RF spectrum for a source with 140-dB/Hz RIN (averaged over 20 simulations). This amount of RIN has a similar effect to 100 kHz of linewidth, giving an electrical SNR of better than 40 dB. The optical SNR was around 20 dB. Note that the wide-band RIN from the laser pollutes all channels in the optical spectrum. The RF intensity fluctuations are caused by the RIN at the frequency of the nth

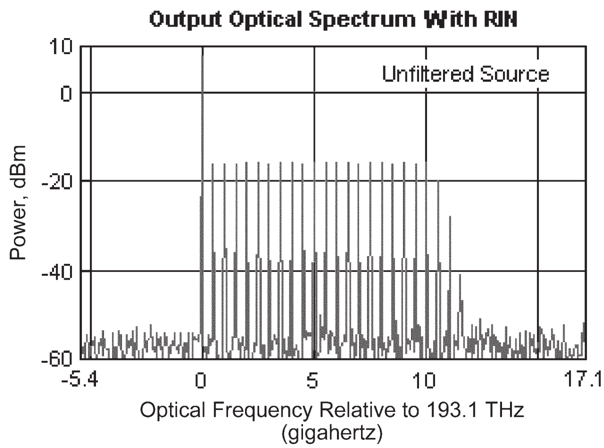

Fig. 11. Optical spectrum for −140 dB/Hz laser RIN.

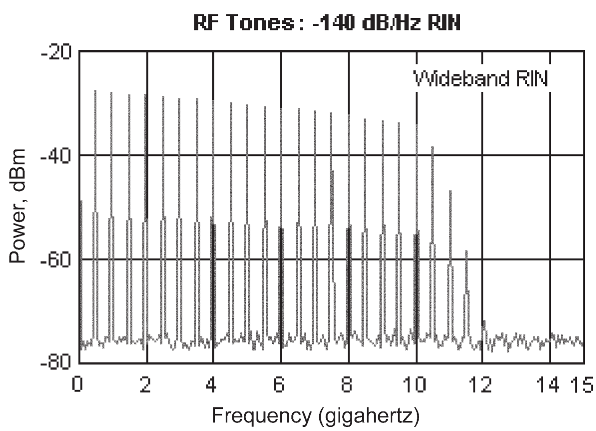

Fig. 12. RF spectrum for −140 dB/Hz laser RIN (unfiltered).

shifted line mixing with the laser line to give electrical RIN around the nth RF tone.

An improvement can be gained using an optical filter at the laser's output, to remove out-of-band RIN, so it is not fed into the loop. Fig. 13 shows the effect on the RF spectrum from using a 500-MHz optical filter after the laser. The SNR is improved by more than 25 dB (close to the ratio of the laser and shifted line powers). Note that the RIN of the dc term is higher, which extends to 250 MHz, because this is produced by the mixing of the strong laser line with the noise surrounding it. A narrow-linewidth source is required, so that linewidth is not converted to intensity fluctuations by the filter.

E. Modulation Waveform Shape

Johnson and Cox [10] used analytical theory and experimentation to show the critical nature of the quality of the sawtooth. They identified fast flyback times, and hence a high electrical bandwidth, as keys to spurious-free spectra. For a 40-dB rejection, the fall time should be less than 1% of the rise time, demanding a bandwidth of 35 times the modulation rate.

Fig. 14 shows the optical spectrum when a perfect sawtooth is filtered with a 5-GHz bandwidth first-order low-pass electrical filter. The optical spectrum has lines that have been down-shifted in optical frequency, due to the flyback portion of the sawtooth having a finite rise time. There is also a shallow null in the positively shifted portion of the spectrum at 6 GHz, and a deep null at 11.5 GHz. These nulls cause a similar null in the RF spectrum, as shown in Fig. 15. There will obviously be some contributions to the RF tones from the negatively shifted RF tones mixing with the laser line, to produce positive RF components. These will also perturb the phases and amplitudes of the RF tones.

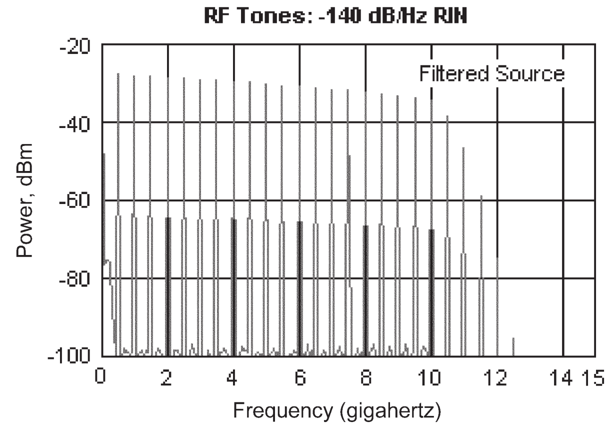

Fig. 13. RF spectrum for −140 dB/Hz laser RIN (filtered source).

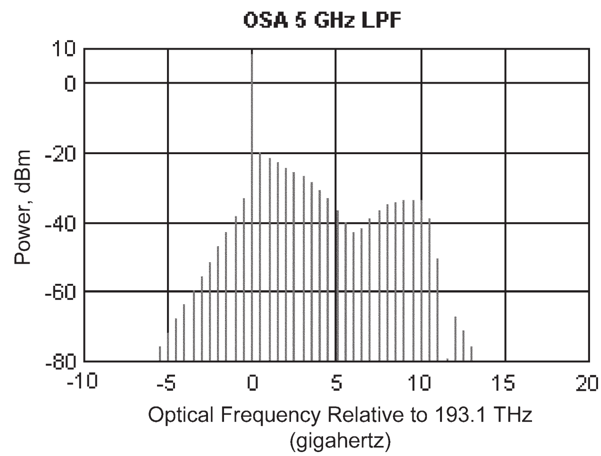

Fig. 14. Optical spectrum with a 5-GHz electrical bandwidth.

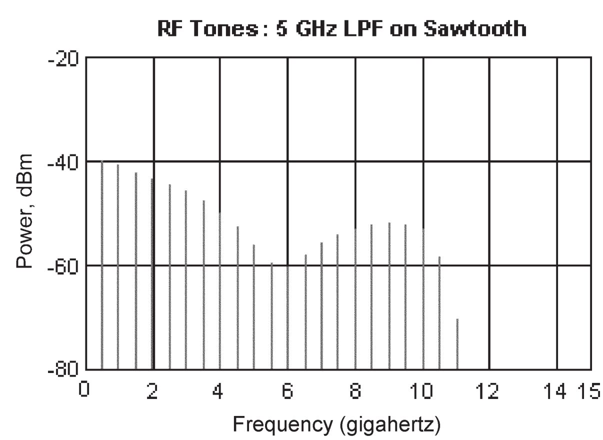

Fig. 15. RF spectrum resulting from the detection of the optical spectrum in Fig. 14.

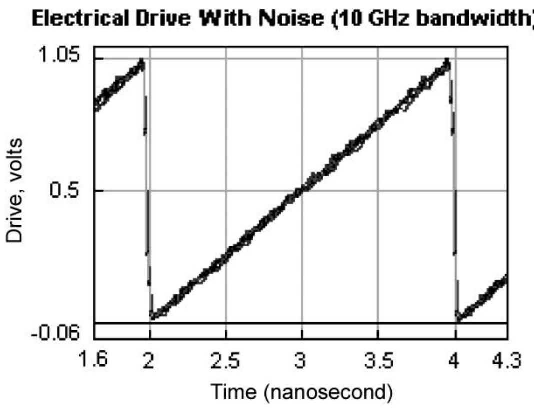

Fig. 16. Sawtooth "eye diagram" showing the magnitude of the electrical noise.

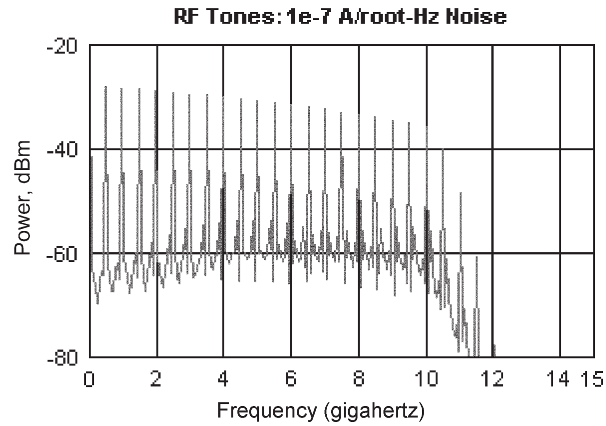

Fig. 17. Effect of electrical noise on the RF tones.

F. Modulation Waveform Noise

The sawtooth generator and subsequent amplifiers will introduce electrical noise into the drive to the phase modulator, and this will convert to a random optical modulation. Fig. 16 shows a signal with a noise density of 0.1 μV per root-hertz (filtered with a 10-GHz first-order low-pass filter, to give a root-mean-square variation of approximately 15 mV). This electrical noise produces the noise floor in the RF spectrum shown in Fig. 17 and also broadens the RF tones due to the optical phase modulation transferring to electrical phase modulation. This illustrates that any electrical noise driving the phase modulator (such as from amplifiers, power supplies, or electromagnetic coupling) will degrade the performance of the system significantly.

G. Loop Phase Matching

An important design issue is how stable the phase length of the fiber loop has to be. An ideal loop would have a zero fluctuation in phase length with time, so that each optical line would have a constant optical phase (because there would be a constant path from source to shifted output). This is illustrated in the unwound loop model of Fig. 18, by setting $e_1 = e_2 = e_3 = e_4 = \cdots$. For zero fluctuation, the phase differences between pairs of optical lines will be equal, so that all pairs of lines will produce an RF contribution with the same phase as other contributions, giving a strong RF tone. However, if the phase errors are unequal along the optical path (due to fluctuations in phase in the path of the modulator), then each RF contribution (from the mixing of a pair of optical lines) could have a different phase, resulting in a weaker (or fluctuating) RF tone. In addition, the RF tone will acquire phase noise from the optical phase fluctuations, even if there is a single contribution (e.g. with weak couplers). For example, the optical line in bold gray (arrowed) could mix with the laser line to give a single RF tone. At time t_3, this line has a phase error of $(e_1 + e_2 + e_3)$. However, at time t_4, it has a phase error of $(e_2 + e_3 + e_4)$. Thus, if $e_1 \neq e_4$, then there will be a phase jump between t_3 and t_4. This will cause a corresponding phase jump in the RF tone.

A common situation will be a slow variation in phase with time relative to the loop delay. This was simulated by driving a second phase modulator with a ramp, incrementing once per loop delay. Fig. 19 shows superimposed RF spectra (only the peaks are shown, as the loop delay and the Fourier transform windows have been reduced to 2 ns) for ramp rates of 0–20° per circulation. These drifts cause dramatic alterations to the RF spectrum: With drifts of $> 4°$ per circulation, the RF spectrum is flattened, but more unpredictable. This is because the phases of the multiple contributions to each RF tone are displaced. Note that the 10-GHz tone has only one contribution (apart from some leakage from the optical filter), and so has the least variation, but the 500-MHz tone is composed of the mixing produced by many pairs of lines, and so has the most variation. A secondary effect of large drifts is that the electrical waveform becomes chirped. This is because each RF tone sees a phase shift proportional to its frequency. This could be a useful method of producing controllable high-bandwidth chirped RF waveforms.

Fig. 20 shows the same simulation but with 50% couplers. The variation of RF power with drift rate is more than 30 dB, and there is a possibility of deep nulls occurring when the vector sum of the RF contributions to an RF tone is equal to zero. Obviously, the design with a dominant laser line (low coupling ratio) is far less sensitive to phase drift than a system with equal powers across the optical spectrum. Interestingly, a flatter RF spectrum may result from allowing (or inducing with a slow phase modulation) phase drift into the system, with the penalty of increased intensity noise in each tone. As most measurements that use averaging, it is possible that this intensity noise has yet to be observed experimentally.

H. Optical Amplifier

The amplifier compensates for the loop loss to maintain a flat optical spectrum. However, it will also induce broadband amplified spontaneous emission (ASE) noise into each circulation, which will itself be shifted on each circulation towards the higher optical frequencies. The simulation assumed an amplifier noise figure of 8 dB, which is far worse than commercially available (around 5 dB), and so represents an amplifier with poor input coupling. Fig. 21 shows the effect on the RF noise floor of the shifted optical noise. The absolute

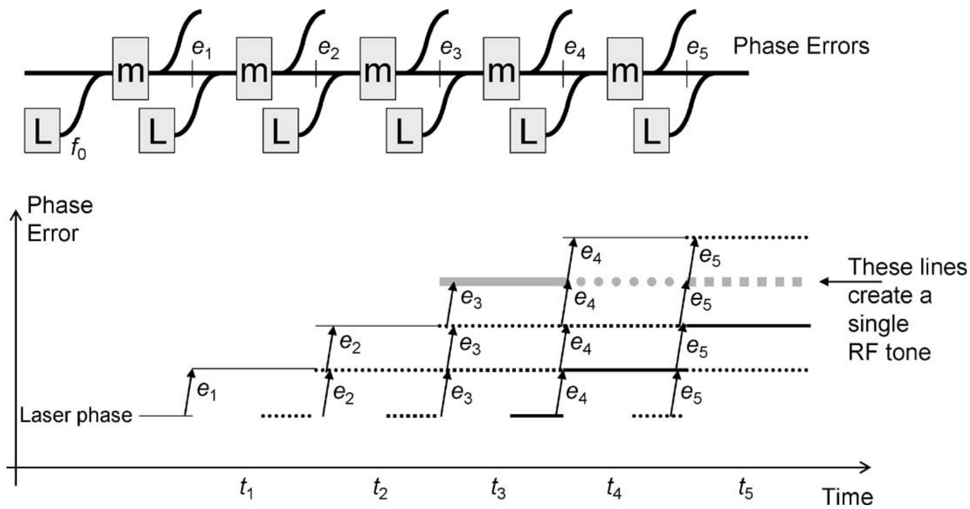

Fig. 18. Unwound ring model with phase errors along the path. If the phase errors are constant ($e_1 = e_2 = e_3 = \cdots$), then a particular optical line will have a constant phase with no discontinuities, as shown in the graph.

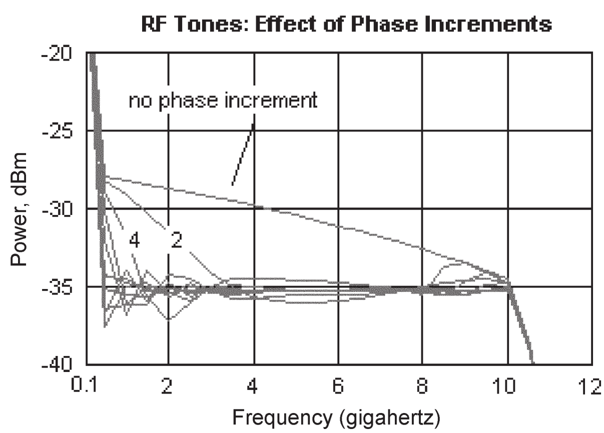

Fig. 19. Effect of incrementing optical phase per circulation (20% couplers). Label is degrees increment per circulation.

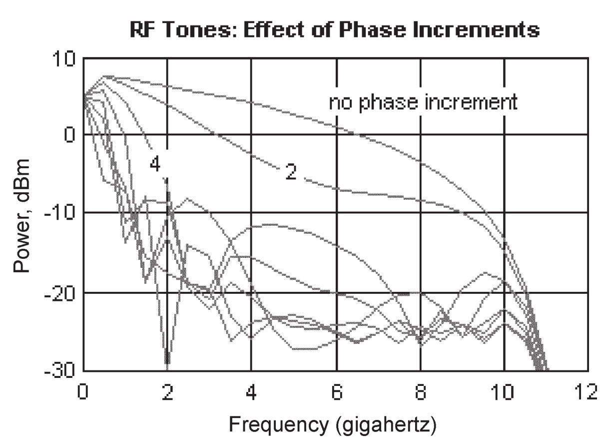

Fig. 20. Effect of incrementing optical phase per circulation (50% couplers). Label is degrees increment per circulation.

noise level is far below the noise caused by other mechanisms (as the gain is low). However, the noise increases for the highest frequency RF tones because of the frequency shifting of the optical noise in the optical domain.

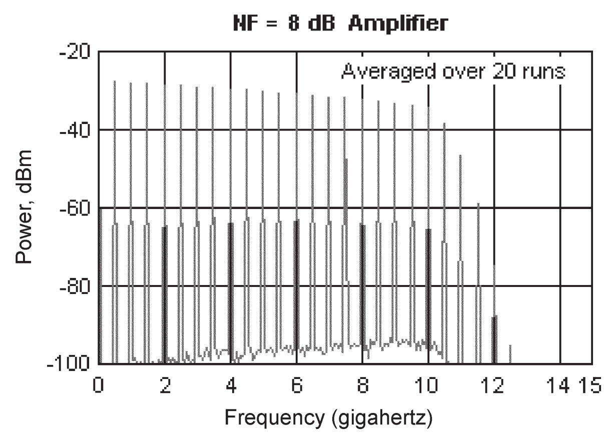

Fig. 21. RF noise due to frequency-shifted optical amplifier noise.

IV. Discussion and Conclusion

The topology change from previous designs, from a single four-port optical coupler to four three-port couplers, allows the strength and phase of the laser line to be adjusted relative to the shifted lines. A strong laser line, compared with the shifted lines, gives a flatter RF comb, because the dominant contribution to each tone is the laser line mixing with a shifted line. Simulations including a drifting optical phase in the loop showed that a strong laser line also reduces the variation in RF tone power due to phase fluctuations. Thus, the new topology has definite advantages to previous designs, although the RF power is significantly weaker.

The performance of the comb generator is dependent on the characteristics of the individual components. The most critical component, as identified previously by Johnson and Cox, is the sawtooth generator driving the phase modulator. This has to have a fast flyback, and also sharp discontinuities between the rising ramp and the flyback portions of the sawtooth waveform. Noise on the waveform seems less important than a large electrical bandwidth, but it does translate to electrical phase noise on the RF tones (which is a critical performance measure for RF signals). The second most important component is the phase stability of the laser source (its linewidth). A laser with a linewidth less than 100 kHz is desirable for an SNR greater than 40 dB.

If a strong laser line is used (weak coupling case), then the broadband noise floor caused by the RIN from the laser will be significant compared with the optical powers of the shifted lines at the frequencies of the lines, and so will convert to RF by mixing with the laser line producing a high RF noise floor. In effect, the RIN of a shifted tone is degraded by the ratio of the laser line to the shifted line power. However, using a filtered laser source reduces the broadband RIN close to the optical tones, so the tones effectively have the same RIN as the source.

The ASE from the optical amplifier has little effect on the performance of the systems, because the amplifier gain is low. However, systems with more recirculations may suffer further degradation and coloring of the RF noise spectrum due to frequency translation of the ASE noise on each recirculation.

In conclusion, simulations have shown the sources of degradation in a serrodyne comb generator and have also suggested and verified an alternative circuit topology using a strong laser line compared with the shifted line powers. The simulations also showed that this new operating regime suffers from degraded RIN performance unless the source is filtered, but is less sensitive to drifts in the optical phase of the loop.

ACKNOWLEDGMENT

The author would like to thank the specification, modeling, and development teams at VPIsystems for their continuing efforts to provide design tools for photonic systems.

REFERENCES

[1] S. Bennett, B. Cai, E. Burr, O. Gough, and A. J. Seeds, "1.8-THz bandwidth, zero-frequency error, tunable optical comb generator for DWDM applications," *IEEE Photon. Technol. Lett.*, vol. 11, no. 5, pp. 551–553, May 1999.

[2] S. Fukushima, C. F. C. Silva, Y. Muramoto, and A. J. Seeds, "Optoelectronic millimetre-wave synthesis using an optical frequency comb generator, optically injection locked lasers, and a unitravelling-carrier photodiode," *J. Lightw. Technol.*, vol. 21, no. 12, pp. 3044–3051, Dec. 2003.

[3] M. Shen and R. A. Minasian, "Photonics-based optical frequency comb generation," in *Conf. Proc. CD-ROM, Australian Conf. Optical Fibre Communications (ACOFT/AOS'04)*, Canberra, Australia, pp. 1–3 [Online]. Available: www.acoft-aos.org. ISBN 0-7315-5222-9 Australian National University.

[4] A. Goutzoulis and K. Davies, "Hardware-compressive 2-D fiber optic delay line architecture for time steering of phased-array antennas," *Appl. Opt.*, vol. 29, no. 36, pp. 5353–5359, 1990.

[5] R. A. Minasian and K. E. Alameh, "Optical-fiber grating-based beamforming network for microwave phased arrays," *IEEE Trans. Microw. Theory Tech.*, vol. 45, no. 8, pp. 1513–1518, Aug. 1997.

[6] K. P. Ho and J. M. Kahn, "Optical frequency comb generator using phase modulation in amplified circulating loop," *IEEE Photon. Technol. Lett.*, vol. 5, no. 6, pp. 721–725, Jun. 1993.

[7] K. K. Wong and R. M. De La Rue, "Electrooptic-waveguide frequency translator in $LiNbO_3$ fabricated by proton exchange," *Opt. Lett.*, vol. 7, no. 11, pp. 546–548, 1982.

[8] M. Izutsu, S. Shikama, and T. Sueta, "Integrated optical SSB modulator/frequency shifter," *IEEE J. Quantum Electron.*, vol. QE-17, no. 11, pp. 2225–2227, Nov. 1981.

[9] I. Tomita, H. Sanjoh, E. Yamada, and Y. Yoshikuni, "Novel method for generating multiple wavelengths by pulsed serrodyne modulation," *IEEE Photon. Technol. Lett.*, vol. 15, no. 9, pp. 1204–1206, Sep. 2003.

[10] L. Johnson and C. Cox, "Serrodyne optical frequency translation with high sideband suppression," *J. Lightw. Technol.*, vol. 6, no. 1, pp. 109–111, Jan. 1988.

[11] A. J. Lowery *et al.*, "Multiple signal representation of photonic devices, systems and networks," *IEEE J. Sel. Top. Quantum Electron.*, vol. 6, no. 2, pp. 282–296, Mar./Apr. 2000.

[12] A. J. Lowery, "Effect of laser intensity and frequency noise on an optical signal processing circuit," in *Conf. Proc. CD-ROM, Australian Conf. Optical Fibre Communications (ACOFT/AOS)*, Canberra, Australia, Jul. 5–8, 2004 [Online]. Available: www.acoft-aos.org. ISBN 0-7315-5222-9 Australian National University.

Arthur Lowery (M'91–SM'96) was born in Yorkshire, England, on 1961. He received the B.Sc. degree (First Class) in applied physics from the University of Durham, U.K., in 1983, and the Ph.D. degree in electrical and electronic engineering from the University of Nottingham, U.K., in 1988.

From 1983 to 1984, he worked at Marconi Radar Systems Ltd., U.K. In 1984, he joined the University of Nottingham as a Lecturer and pioneered the time-domain field modeling of semiconductor lasers as the transmission-line laser model. In 1990, he emigrated to Australia to become a Senior Lecturer at the newly-formed Photonics Research Laboratory at the University of Melbourne. After working on photonic computer-aided design (CAD), packet switching, and laser ranging, he was promoted to Associate Professor and Reader in 1993. He continued to develop novel time-domain simulation techniques and to lead collaborative research as a Fellow of the Australian Photonics Cooperative Research Centre. In 1996, he co-founded Virtual Photonics Pty. Ltd., with Phil Gurney. In 1995, Optoelectronic, Photonic and Advanced Laser Simulator (OPALS) was released, followed by Gigabit Optical Link Designer (GOLD). Virtual Photonics merged with BNeD, Berlin, Germany, in 1998, with him as the Chief Technology Officer (CTO), leading the development of VPI's physical-level photonic design automation tools such as VPItransmissionMaker and VPIcomponentMaker, which are widely used in the industry and academia for development, research, and teaching. In 2004, he was appointed Professor of Electrical and Computer Systems Engineering at Monash University, Melbourne, Australia, where he is working on active photonic circuits, electromagnetic design automation, and the applications of photonic technology. He has published more than 170 papers and four book chapters on the simulation of photonic devices and circuits and photonic applications such as mode locking, packet switching, transmission systems, and high-speed circuits.

Prof. Lowery is Fellow of the Institution of Electrical Engineers, U.K.